
EFDA–JET–PR(03)34

L.-G. Eriksson, T. Johnson, T. Hellsten, C. Giroud, V.G. Kiptily, K.Kirov,
J. Brzozowski, M. DeBaar, J. DeGrassie, M. Mantsinen, A. Meigs,
J.-M. Noterdaeme, A. Staebler, A. Tuccillo, K.-D. Zastrow
and JET EFDA contributors

Plasma Rotation Induced by Directed Waves in the Ion Cyclotron Range of Frequencies

Plasma Rotation Induced by Directed Waves in the Ion Cyclotron Range of Frequencies

L.-G. Eriksson, T. Johnson¹, T. Hellsten¹, C. Giroud², V.G. Kiptily³, K.Kirov⁴,
J. Brzozowski¹, M. DeBaar², J. DeGrassie⁶, M. Mantsinen⁷, A. Meigs³,
J.-M. Noterdaeme^{4,5}, A. Staebler⁴, A. Tuccillo⁸, K.-D. Zastrow³
and JET EFDA contributors*

Association EURATOM-CEA, CEA/DSM/DRFC, CEA-Cadarache, F-13108 St. Paul lez Durance, France

¹Euratom-VR Association, Stockholm, Sweden

²The Stichting voor Fundamenteel Onderzoek der Materie FOM, The Netherlands

³Association Euratom-UKAEA Culham, Science Centre, Abingdon, United Kingdom

⁴Max-Planck IPP-EURATOM Assoziation, Garching, Germany

⁵Gent University, Department EESA, Belgium

⁶General Atomics, USA;

⁷Helsinki University of Technology, Association Euratom-Tekes, Finland

⁸Associazione Euratom-ENEA sulla fusione, Frascati, Italy

** See annex of J. Pamela et al, "Overview of Recent JET Results and Future Perspectives",
Fusion Energy 2002 (Proc. 19th Int. Conf. Lyon, 2002), IAEA, Vienna*

“This document is intended for publication in the open literature. It is made available on the understanding that it may not be further circulated and extracts or references may not be published prior to publication of the original when applicable, or without the consent of the Publications Officer, EFDA, Culham Science Centre, Abingdon, Oxon, OX14 3DB, UK.”

“Enquiries about Copyright and reproduction should be addressed to the Publications Officer, EFDA, Culham Science Centre, Abingdon, Oxon, OX14 3DB, UK.”

ABSTRACT

Change of the toroidal plasma rotation induced by directed waves in the Ion Cyclotron Range of Frequencies (ICRF) has been identified experimentally for the first time on the JET tokamak. The momentum carried by the waves is initially absorbed by fast resonating ions, which subsequently transfer it to the bulk plasma. Thus, the results provide evidence for the influence of ICRF heated fast ions on plasma rotation.

Plasma rotation can have beneficial effects on the performance of tokamak plasmas. In particular, rotation can influence the MHD stability and increase the stabilising effect of a resistive wall [1]. Furthermore, it is believed that the shear in the toroidal velocity component associated with the radial electric field can suppress turbulence and thereby create transport barriers, see e.g. [2, 3]. It is therefore important to investigate mechanisms that can induce plasma rotation.

In present day tokamak experiments, the momentum imparted by Neutral Beam Injection (NBI) induces significant toroidal plasma rotation. However, there is limited scope for controlling the location and direction of the torque. Greater flexibility in this respect could be achieved by absorption of directed (or travelling) waves in the Ion Cyclotron Range of Frequencies (ICRF). Such waves provide globally much less torque than NBI injected ions. Nevertheless, the peak torque density provided by the waves would not necessarily be small since the power deposition tends to be much narrower for ICRF heating than for NBI. Since the absorption is concentrated to the vicinity of the cyclotron resonance, $\omega = \omega_{ci}(R)$, of the resonating ion species in the plasma, the spatial location of the peak of the torque density can be varied by changing the frequency (n is the harmonic number of the interaction, and R is major radius of the tokamak). The influence of directed waves has been discussed theoretically in e.g. Ref. [4]. Furthermore, measurements of rotation profiles in plasmas with directed ICRF waves have been reported in [11]. However, the experiments were not designed for detecting the influence of directed waves on rotation. The cyclotron resonance was placed fairly far off-axis and the applied ICRF power was rather low. Under these conditions the predicted influence on rotation is small, and indeed only very minor differences were detected between plasmas with co and counter current propagating waves.

In this paper we present the first clear experimental evidence for the influence of absorbed wave momentum, carried by ICRF waves, on plasma rotation in a tokamak. Fast resonating ions act like an intermediary in the process, they first absorb the wave momentum, and subsequently transfer it to the bulk plasma via collisions and by being displaced radially. Thus, our results provide evidence for the influence of fast ICRF heated ions on plasma rotation.

The mechanisms behind the transfer of momentum from the waves to the resonating ions and subsequently to the background plasma are briefly summarized below.

An ion absorbing a wave quantum changes its energy by $\Delta E = \eta\omega$, and there is also a concomitant change in its toroidal angular momentum $\Delta P_\phi = \eta k_\phi R = \eta N$, where N is the toroidal mode number. Equivalently, $\Delta P_\phi = (N/\omega) \Delta E$. Obviously, the same result can be obtained from

combining the equation of motion for a particle with Maxwell's equation. Thus, the rate at which the waves impart toroidal angular momentum to the plasma is given by, $\sum_N (N/\omega) P_{ICRF}(N)$, where $P_{ICRF}(N)$ is the power coupled by the antennas for a toroidal mode number N . The fast ions transfer the momentum to the bulk plasma via two mechanisms, collisions and a radial fast ion current. In the latter case, the plasma strives to preserve quasi neutrality. As a result, the fast ion radial current is compensated for by an opposite current in the bulk plasma, and there is consequently a $j \times B$ force on the bulk plasma. One can show that a fast ion current directed outwards produces a counter-current torque on the bulk plasma, whereas an inward fast ion current creates a co-current torque. In the presence of waves directed in the toroidal direction of the plasma current, the wave particle interaction leads to a drift of turning points of resonating trapped ions towards the equatorial plane [5, 6], and many of these ions will eventually de-trap into co-passing orbits in the potato regime [5, 7, 8,]. Consequently, the momentum imparted to the bulk plasma in this case can be dominated by collisions with co-passing ions in the potato regime and the inward fast ions current of trapped resonating ions. On the other hand, in the case of waves propagating counter to the current, the turning points of resonating trapped fast ions are driven away from the equatorial plane, and the momentum is largely transferred via the associated outward current of fast ions.

Before we turn to the experimental results and their analysis, let us first briefly discuss a few important points concerning the experimental set up and the key diagnostic measurements. The JET tokamak is equipped with four ICRF antennas, and each antenna has four current carrying straps. The currents in the straps can be phased relative to each other, and in the experiments reported here the phase difference between two neighbouring straps was either $+90^\circ$ or -90° . The $+90^\circ$ phasing produces waves propagating predominantly in the co-current direction and -90° phasing produces waves in the opposite direction. Typical toroidal mode number spectra for $+90^\circ$ or -90° phasing can be found in Ref. [9]. The locations of the peaks of these spectra are relatively insensitive to the heating scenario, and they appear roughly at $N=\pm 12$ for $\pm 90^\circ$ phasing. Thus, given that the toroidal mode number spectrum is relatively fixed, one can maximize the toroidal momentum carried by the waves by using a low frequency scenario. Fundamental minority heating of ^3He in a deuterium plasma, (^3He)D ($n_{\text{He}}/n_{\text{D}} \sim 1-3\%$) with $f=37\text{MHz}$ was chosen for the experiments, the current and field were of 1.8MA and 3.4T, respectively. For these parameters the ^3He cyclotron resonance was located slightly on the high field side ($\sim 15\text{cm}$).

A perturbative technique, in which a diagnostic beam was fired into the plasma for short periods (200ms, so called beam blips), was used to measure the toroidal rotation profile. It was deduced from the Doppler shift of the active charge exchange spectrum for C^{+6} [10]. As discussed in detail in [11], by considering only the first spectrum taken after the application of a beam blip, the effects of the perturbation imparted by the injected ions should be small and the measured rotation profile a fair reflection of the profile before the beam blip. Furthermore, we will here chiefly consider differences between discharges. As a result, we are less sensitive to any

perturbations introduced by the diagnostic beam since they would be similar in all the discharges.

The gamma-ray profile monitor installed on the JET tokamak has nine vertical and ten horizontal lines of sight [12]. Is a powerful tool for diagnosing fast resonating ions. Especially reactions produced by fast ^3He ions interacting with carbon and beryllium impurities in the plasma are well established in this respect. For the present experiments, the gamma-ray monitor provided important information on the topological properties of fast ion orbits.

An overview of essential discharge parameters is shown for two discharges, $+90^\circ$ and -90° phasing respectively, in Fig.1. The applied ICRF power, NBI diagnostic blips and plasma central density were virtually equal in the two ICRF only discharges. There are small differences in the stored energies and somewhat larger differences in the central electron temperature. These differences are consistent with an inward/outward drift of the fast ions during heating with $+90^\circ$ / -90° phasing [5-8]. The measured toroidal rotation profiles for the discharges taken at the beginning of the beam blip applied at 51 sec are shown in Fig.2. The profiles show plasma rotation in the co-current direction. However, there is a substantial difference between them, the discharge with $+90^\circ$ phasing rotates significantly faster in the co-current direction than the -90° discharge. Since the $+90^\circ$ phasing produces waves propagating in the same toroidal direction as the current, this result is qualitatively consistent with a transfer of the absorbed wave momentum from the resonating fast ions to the bulk plasma. To further increase the confidence in the identification of the differences as being due to the absorbed wave momentum, we have added in Fig. 2 the rotation profile from a $+90^\circ$ discharge where 2MW ICRF power has been replaced by 2MW of Lower Hybrid (LH) power in the high power heating phase. As can be seen, the rotation profile for this discharge lies in between the other two. The LH waves are directed, but for the same amount of power they only carry about 10% of the momentum of the $+90^\circ$ ICRF waves. The discharge with 2MW of LH power had a lower stored energy (about 5-10%) than the other two, which is not unexpected since LH heating provides direct electron heating, i.e. no fast ions, and deposits the power further off-axis than the ICRF heating. From these facts we conclude that the stronger central rotation in the $+90^\circ$ discharge is not due to improved central heating and/or a higher stored energy (otherwise the discharge with LH heating should have rotated less than the -90° discharge). Thus, we can be fairly confident that the difference in rotation profiles between the $+90^\circ$ and -90° ICRF only discharges is due to the absorbed wave momentum and the concomitant differences in the fast ion characteristics. Thus, there is an underlying mechanism giving rise to a co-current rotation, and overlaid on this we have the torque imparted to the plasma by the absorption of wave momentum. The effect of the latter is consistent both qualitatively and, as we show below, quantitatively with the observed difference in rotation velocity between the $+90^\circ$ and -90° discharges.

We now turn to the behaviour of the fast resonating ions. The signals from the seven central lines of sights of the gamma-ray detector, normalised to their highest value, as a function of the major radius where the sight line crosses the mid-plane are shown in Figs. 3 and 4 for the two

discharges with $+90^\circ$ and -90° phasing. In the discharge with $+90^\circ$ phasing the emission is slightly displaced towards the low field side of the magnetic axis, and it has an almost symmetrical shape. By contrast, the -90° discharge has a more asymmetrical emission, weighted towards the high field side, c.f. [6, 8]. The asymmetrical emission for the -90° discharge is consistent with a strong population of fast trapped ions with turning points on the high field side. Such ions spend most of their time close to their turning points, and their contribution to the emission is therefore strongest on the high field side. On the other hand, because of the symmetrical shape of the emission for the $+90^\circ$ case, one can conjecture that it is dominated by contributions from fast passing ions in the potato regime [13]. The presence of such ions is consistent with theoretical expectations [5, 7]. Thus, the theoretical picture discussed above appears to be at least qualitatively correct. The co-current torque in the centre during heating with $+90^\circ$ phasing is mainly transferred to the bulk plasma by collision with fast passing ions in the potato regime and the inward drift (towards smaller minor radii) of trapped ions, whereas an outward current of trapped ions plays a key role for the counter-current torque during heating with -90° phasing. It should be noted that ions on co-current passing orbits in the potato regime play an important role also in theories [14-16] attempting to explain observations [11, 17-21] of co-current toroidal rotation in plasmas with little or no imparted momentum. These theories [14-16] are based on fast ion effects and often rely on the presence of ions on such orbits for producing the necessary central co-current torque

We have used the SELFO code [22] to assess if the experimental results are in quantitative as well as qualitative agreement with theoretical expectations. It calculates the ICRF power deposition and the distribution function of the resonating ions self-consistently. A momentum transport equation is also needed. Owing to a lack of information on the details of the momentum transport in the plasma (likely to be anomalous), we have to use a simple, but still reasonable model, viz., $n_i m_i \partial V_\phi / \partial t = g^{-1/2} (\partial / \partial \rho) [g^{-1/2} n_i m_i D \partial V_\phi / \partial \rho] + t$ where V_ϕ is the rotation velocity, m_i and n_i are the masses and densities of the plasma ion species (summation over repeated indexes is assumed), ρ is a radial coordinate, $g^{-1/2}$ is the Jacobian, t is the torque density provided by the fast ions, D is a momentum diffusion coefficient taken to be constant and equal to $a^2 / (\alpha_M \tau_M)$, a is the minor radius of the plasma, τ_M is the momentum confinement time, and α_M is a parameter adjusting the transport so that the global confinement time is obtained (in reality α_M depends on the rotation profile, but it should be of the order of 5). Experimental data have been used in the simulations with the SELFO code. Inserting the simulated torque density into the momentum diffusion equation assuming $\tau_M = \tau_E \approx 0.3$ (τ_E is the measured energy confinement time), and $\alpha_M = 3$, results in the difference in rotation velocity between the two discharges displayed in Fig.4. The central difference is of the order of 4 krad/s, in good agreement with the experimental value.

The characteristics of the resonating fast ions in the SELFO simulation are also broadly consistent with the experimental gamma-ray emission. The fast ion distribution function calculated by SELFO has been used to simulate the response of the seven central gamma-ray detectors, the results have been added to Figs.3 and 4. The spatial distribution of the measured and calculated

gamma-rays have very similar features. Only in the relative level is there a difference, the ratio between of the emissions at the normalisation points for $+90^\circ$ and -90° phasing is roughly 4 experimentally and 2 in the SELFO simulations. This is probably due to a too low central concentration of ^3He ions in the centre of the plasmas in the $+90^\circ$ simulation, caused by the pump out of resonating ions and a too weak transport of thermal ^3He ions (there is no anomalous particle transport of thermal ions in SELFO). Furthermore, an increase of the ^3He concentration in the SELFO simulation for the -90° case brings down the gamma-ray emission to the experimental level with only a very marginal change in the rotation. The calculations confirm that the peak of the emission on the high field for the -90° discharge is due to resonating trapped ions. Furthermore, the symmetric emission, with respect to the magnetic axis, for the $+90^\circ$ case can in the simulations be clearly identified as being due to co-current passing orbits in the potato regime, indicating how important they can be for providing a central co-current torque.

SUMMARY

In summary, we have presented evidence for ICRF induced bulk plasma rotation during heating with directed waves in the JET tokamak, and we have discussed the key role played by the fast resonating ions in transferring the absorbed momentum to the background plasma.

ACKNOWLEDGEMENTS

This work has been performed under the European Fusion Development Agreement. The work carried out by UKAEA personnel was partly funded by the U.K. Department of Trade and Industry and EURATOM.

REFERENCES

- [1]. A.M. Garofalo, et al., Nuclear Fusion **41**, 1171 (2001).
- [2]. T.S. Hahm and K.H. Burrell, Physics of Plasmas **2**, 1648 (1995).
- [3]. E.J. Synakowski, Plasma Physics and Controlled Fusion **40**, 581 (1998).
- [4]. F.W. Perkins, R.B. White and V.S. Chan, Physics of Plasmas **9**, 511 (2002).
- [5]. T. Hellsten et al., Phys. Rev. Lett. **74**, 3612 (1995).
- [6]. L.-G. Eriksson, et al., Phys. Rev. Lett. **81**, 1231 (1998).
- [7]. J. Hedin, T. Hellsten and L.-G. Eriksson, Nuclear Fusion **42**, 527 (2002).
- [8]. M.Mantsinen, et al., Phys. Rev. Lett. **89**, 115004-1 (2002).
- [9]. A. Kaye, et al., Fusion Engineering and design **24**, 1 (1994).
- [10]. H. Weissen et al., Nuclear Fusion **29**, 287 (1989).
- [11]. J.-M. Noterdaeme et al., Nuclear Fusion **43**, 274 (2003).
- [12]. O.N. Jarvis et al., Nuclear Fusion **36**, 1513 (1996); V.Kiptily, et al., Nuclear Fusion **42**, 999 (2002).
- [13]. L.-G. Eriksson and F. Porcelli, Plasma Phys. and Controlled Fusion **43**, R145 (2001).
- [14]. F.W. Perkins, R.B. White, P.T. Bonoli and V.S. Chan, Phys. Plasmas **8**, 2181 (2001).
- [15]. V. S. Chan, S. C. Chiu and Y. A. Omelchenko, Physics of Plasmas **9**, 501 (2002).
- [16]. L.-G. Eriksson and F. Porcelli, Nuclear Fusion **42**, 959 (2002).
- [17]. L.-G. Eriksson, R. Giannella, T. Hellsten, E. Källne and G. Sundström, Plasma Physics and Controlled Fusion **34**, 863 (1992).
- [18]. L.-G. Eriksson, E. Righi, K.D. Zastrow, Plasma Phys. and Contr. Fusion **39**, 27 (1997).
- [19]. R. Rice, et al., Nuclear Fusion **38**, 75 (1998).
- [20]. R. Rice, et al., Nuclear Fusion **39**, 1175 (1999).
- [21]. L.-G. Eriksson, G.T. Hoang and V. Bergeaud, Nuclear Fusion **41**, 91 (2001).
- [22]. J. Hedin, T. Hellsten, J. Carlsson, Proc. of Joint Varenna-Lausanne Workshop on “Theory of fusion Plasmas” 467, Varenna (1998).

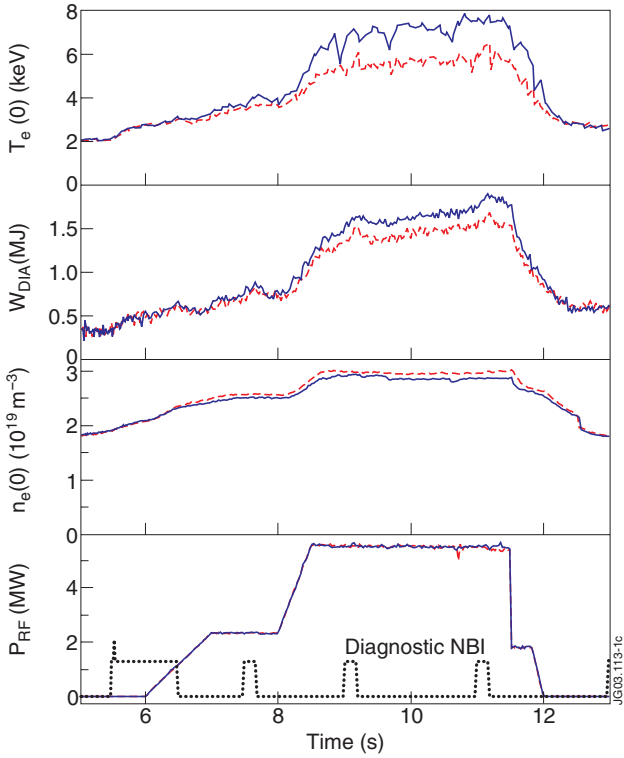


Figure 1: Overview of two discharges using the $(^3\text{He})\text{D}$ heating scheme, one with $+90^\circ$ antenna phasing (Pulse No: 57307), (—), and the other with -90° (Pulse No: 57303), (- - -); (a) Electron temperature (measured by ECE); (b) diamagnetic stored energy; (c) central electron density; (d) ICRF power and NBI power for the diagnostic beam pulses.

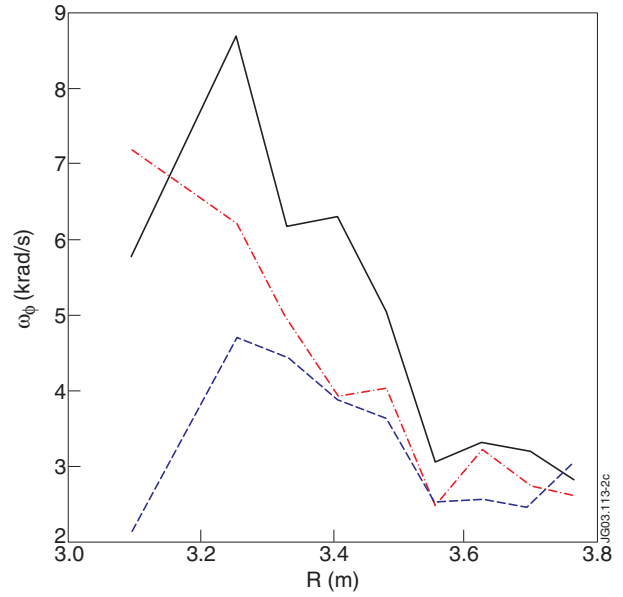


Figure 2: Carbon impurity rotation profiles for the $+90^\circ$, (—), and -90° (- - -) discharges in Fig.1. The profile for a discharge with 2MW of ICRF power exchanged for 2MW of LH power has been added for comparison, (- · - ·).

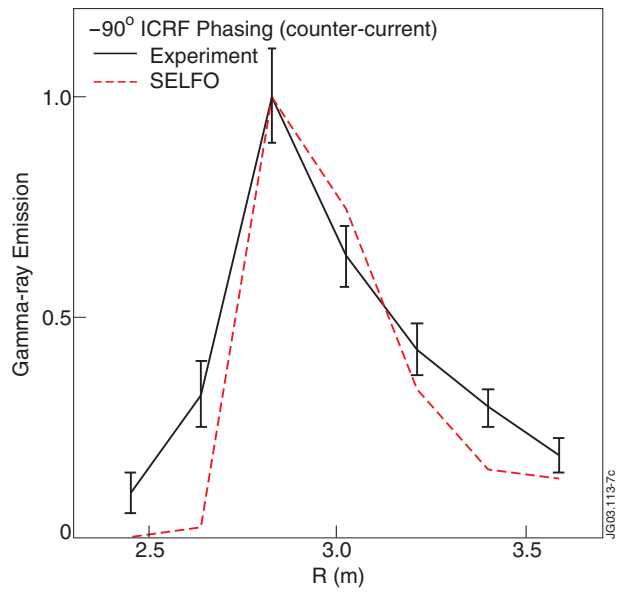
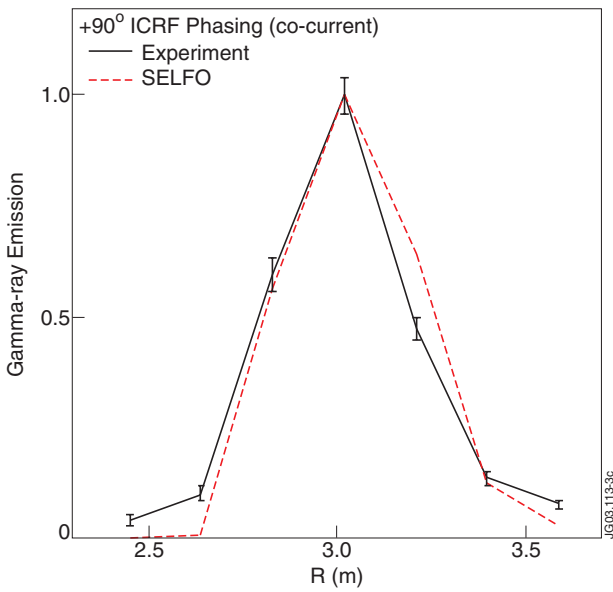


Figure 3: Normalized gamma-ray emission from seven central vertical detectors as a function of the major radius where the sight lines intersects the mid-plane; (a) $+90^\circ$ phasing, (b) -90° phasing; measured (—) and simulated by the SELFO code (- - -).

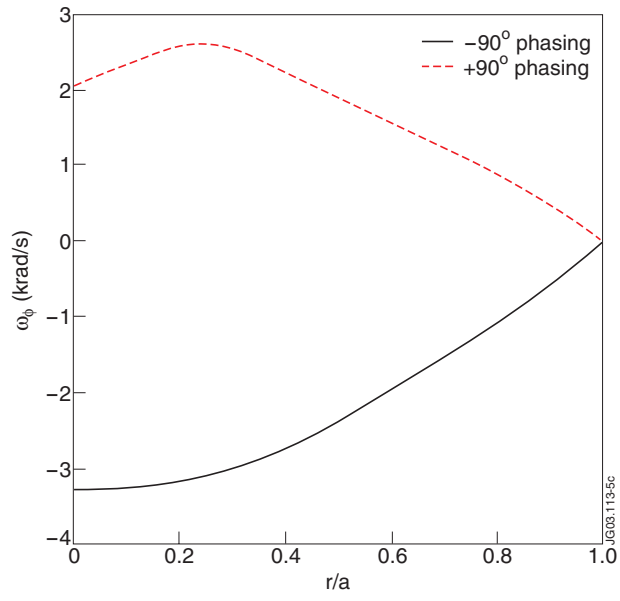


Figure 4: The difference in rotation profile resulting from inserting the torques simulated by the SELFO code in the simple momentum diffusion equation.